



Voronoi-based geometry estimator for 3D digital surfaces

Louis Cuel, Jacques-Olivier Lachaud, Boris Thibert

► **To cite this version:**

Louis Cuel, Jacques-Olivier Lachaud, Boris Thibert. Voronoi-based geometry estimator for 3D digital surfaces. 2014. <hal-00990169>

HAL Id: hal-00990169

<https://hal.archives-ouvertes.fr/hal-00990169>

Submitted on 13 May 2014

HAL is a multi-disciplinary open access archive for the deposit and dissemination of scientific research documents, whether they are published or not. The documents may come from teaching and research institutions in France or abroad, or from public or private research centers.

L'archive ouverte pluridisciplinaire **HAL**, est destinée au dépôt et à la diffusion de documents scientifiques de niveau recherche, publiés ou non, émanant des établissements d'enseignement et de recherche français ou étrangers, des laboratoires publics ou privés.

Voronoi-based geometry estimator for 3D digital surfaces

Louis Cuel^{1,2}, Jacques-Olivier Lachaud¹, and Boris Thibert²

¹ Université de Savoie, Laboratoire LAMA
Le bourget du lac, France

² Université de Grenoble, Laboratoire Jean Kuntzmann
Grenoble, France

Abstract. We propose a robust estimator of geometric quantities such as normals, curvature directions and sharp features for 3D digital surfaces. This estimator only depends on the digitisation gridstep and is defined using a digital version of the Voronoi Covariance Measure, which exploits the robust geometric information contained in the Voronoi cells. It has been proved in [1] that the Voronoi Covariance Measure is resilient to Hausdorff noise. Our main theorem explicits the conditions under which this estimator is multigrid convergent for digital data. Moreover, we determine what are the parameters which maximise the convergence speed of this estimator, when the normal vector is sought. Numerical experiments show that the digital VCM estimator reliably estimates normals, curvature directions and sharp features of 3D noisy digital shapes.

1 Introduction

Differential quantities estimation, surface reconstruction and sharp feature detection are motivated by a large number of applications in computer graphics, geometry processing or digital geometry.

Digital geometry estimators. The common way to link the estimated differential quantities to the exact Euclidean one is the multigrid convergence principle: when the shape is digitized on a grid with *gridstep* h tending to zero, the estimated quantity should converge to the expected one. In dimension 2, several multigrid convergent estimators have been introduced to approach normals [2, 3] and curvatures [3–5]. In 3D, empirical methods for normal and curvature estimation have been introduced in [6]. More recently, a convergent curvature estimator based on covariance matrix was presented in [7].

Voronoi-based geometry estimation. Classical principal component analysis methods try to estimate normals by fitting a tangent plane or a higher-order polynomial (e.g. see [8]). In contrast, Voronoi-based methods try to fit the normal cones to the underlying shape, either geometrically [9] or more recently using the covariance of the Voronoi cells [10, 1]. Authors of [1] have improved the method of [10] by changing the domain of integration and the averaging process. The authors define

the *Voronoi Covariance Measure* (VCM) of any compact sets, and show that this notion is stable under Hausdorff perturbation. Moreover, the VCM of a smooth surface encodes a part of its differential information, such as its normals and curvatures. With the stability result, one can therefore use the VCM to estimate differential quantities of a surface from a Hausdorff approximation such as a point cloud or a digital contour.

Voronoi Covariance measure background. The *Voronoi covariance measure* (VCM) has been introduced in [1] for normals and curvature estimations. Let K be a compact subset of \mathbb{R}^3 and d_K the *distance function* to K , i.e. the map $d_K(x) := \min_{p \in K} \|p - x\|$. A point p where the previous minimum is reached is called a *projection* of x on K . Almost every point admits a single projection on K , thus defining a map $p_K : \mathbb{R}^3 \rightarrow K$ almost everywhere. The *R-offset* of K is the R -sublevel set of d_K , i.e. the set $K^R := d_K^{-1}(] - \infty, R[)$. The VCM maps any integrable function $\chi : \mathbb{R}^3 \rightarrow \mathbb{R}^+$ to the matrix

$$\mathcal{V}_{K,R}(\chi) := \int_{K^R} (x - p_K(x))(x - p_K(x))^{\mathbf{t}} \chi(p_K(x)) dx.$$

Remark that this definition matches the definition introduced in [1]: when χ is

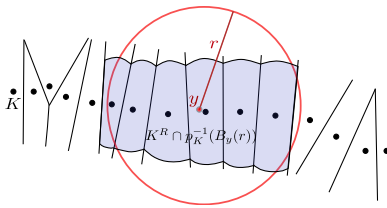


Fig. 1: VCM domain of integration.

the indicatrix of a ball, one recovers a notion similar to the convolved VCM : $\mathcal{V}_{K,R}(\chi) := \int_{K^R \cap p_K^{-1}(B_y(r))} (x - p_K(x))(x - p_K(x))^{\mathbf{t}} dx$. The domain of integration $K^R \cap p_K^{-1}(B_y(r))$ is the offset of K intersected with a union of Voronoi cells (cf. Figure 1). The stability result of [1] implies that information extracted from the covariance matrix such as normals or principal directions are stable with respect to Hausdorff perturbation.

Contributions. The contributions of the paper can be sketched as follows. First, we define the estimator of the VCM in the case of digital data, for which we prove the multigrid convergence (Sect. 2, Theorem 1). We then show that the normal direction estimator, defined as the first eigenvector of the VCM estimator, is also convergent with a speed in $O(h^{\frac{1}{8}})$ (Sect. 3, Corollary 1). Furthermore, Theorem 2 specifies how to choose parameters r and R as functions of h to get the convergence. Finally, we present an experimental evaluation showing that this convergence speed

is closer to $O(h)$ in practice (Sect. 4). Moreover, experiments indicate that the VCM estimator can be used to estimate curvature information and sharp features in the case of digital data perturbed by Hausdorff noise.

2 VCM on digital sets

In this section, we define an estimator of the VCM in the case of 3D digital input. Theorem 1 explicits the conditions under which this estimator is multigrid convergent for digital data.

2.1 Definition

Let X be a compact domain of \mathbb{R}^3 whose boundary is a surface of class C^2 . We denote ∂X the boundary of X , $X_h := Dig_h(X) = X \cap (h\mathbb{Z})^3$ the Gauss digitisation of X , and $\partial_h X \subset \mathbb{R}^3$ the set of boundary surfels of X_h . We define a digital approximation of the VCM on a subset of the point cloud : $Z_h = \partial_h X \cap h(\mathbb{Z} + \frac{1}{2})^3$. For each point $x \in h(\mathbb{Z} + \frac{1}{2})^3$ with $x = (x_1, x_2, x_3)$, we can define the voxel of center x by $\text{vox}(x) = [x_1 - \frac{1}{2}h, x_1 + \frac{1}{2}h] \times [x_2 - \frac{1}{2}h, x_2 + \frac{1}{2}h] \times [x_3 - \frac{1}{2}h, x_3 + \frac{1}{2}h]$. We then define the *digital VCM estimator* as

$$\widehat{V}_{Z_h, R}(\chi) := \sum_{x \in \Omega_h^R} h^3(x - p_{Z_h}(x))(x - p_{Z_h}(x))^t \chi(p_{Z_h}(x)),$$

where $\Omega_h^R = \{x \in Z_h^R \cap h(\mathbb{Z} + \frac{1}{2})^3, \text{vox}(x) \subset Z_h^R\}$ is the set of centers of voxels entirely contained in Z_h^R , the R -offset of Z_h (see Fig. 2). Remark that the Hausdorff distance between ∂X and the point cloud Z_h used in the definition is less than h .

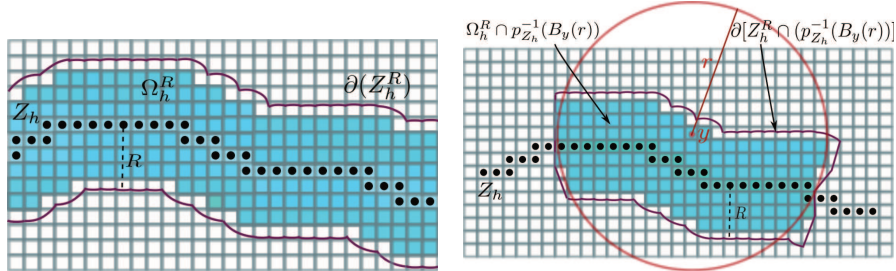


Fig. 2: Digitisation of the offset and its localisation.

2.2 Multigrid convergence of the VCM-estimator

The main theoretical result of the paper is the following theorem. Roughly speaking, it quantifies the approximation of the VCM of a smooth surface by the digital

VCM of its Gauss digitisation. We denote by $\|\cdot\|_{\text{op}}$ the matrix norm induced by the Euclidean metric. Given a function $f : \mathbb{R}^n \rightarrow \mathbb{R}$, we let $\|f\|_{\infty} = \max_{x \in \mathbb{R}^n} |f(x)|$ and denote $\text{Lip}(f) = \max_{x \neq y} |f(x) - f(y)| / \|x - y\|$ its Lipschitz constant.

Theorem 1. *Let X be a compact domain of \mathbb{R}^3 whose boundary ∂X is a C^2 surface with reach $\rho > 0$. Let $R < \frac{\rho}{2}$ and $\chi : \mathbb{R}^3 \rightarrow \mathbb{R}^+$ be an integrable function whose support is contained in a ball of radius r . Then for any $h > 0$ such that $h \leq \min\left(R, \frac{r}{2}, \frac{r^2}{32\rho}\right)$, one has*

$$\begin{aligned} \left\| \mathcal{V}_{\partial X, R}(\chi) - \widehat{\mathcal{V}}_{Z_h, R}(\chi) \right\|_{\text{op}} &= O\left(\text{Lip}(\chi) \times [(r^3 R^{\frac{5}{2}} + r^2 R^3 + r R^{\frac{9}{2}}) h^{\frac{1}{2}}] \right. \\ &\quad \left. + \|\chi\|_{\infty} \times [(r^3 R^{\frac{3}{2}} + r^2 R^2 + r R^{\frac{7}{2}}) h^{\frac{1}{2}} + r^2 R h] \right). \end{aligned}$$

In the theorem and in the following of the text, the constant involved in the notation $O(\cdot)$ only depends on the reach of ∂X and on the dimension (which is three here).

For the proof of Theorem 1, we introduce the VCM of the point cloud Z_h , namely $\mathcal{V}_{Z_h, R}(\chi)$. By the triangle inequality, one has

$$\left\| \mathcal{V}_{\partial X, R}(\chi) - \widehat{\mathcal{V}}_{Z_h, R}(\chi) \right\|_{\text{op}} \leq \left\| \mathcal{V}_{\partial X, R}(\chi) - \mathcal{V}_{Z_h, R}(\chi) \right\|_{\text{op}} + \left\| \mathcal{V}_{Z_h, R}(\chi) - \widehat{\mathcal{V}}_{Z_h, R}(\chi) \right\|_{\text{op}}.$$

In Proposition 1, we bound the second term and in Proposition 2, we bound the first term.

Estimation of the VCM of a point cloud. Here and in the following of this section, X is a compact domain of \mathbb{R}^3 whose boundary ∂X is a C^2 surface with reach $\rho > 0$. We put $R < \frac{\rho}{2}$ and $\chi : \mathbb{R}^3 \rightarrow \mathbb{R}^+$ is an integrable function whose support is contained in a ball $\mathcal{B}_y(r)$ of center y and radius r .

Proposition 1. *For any $h \leq \min\left(R, \frac{r}{2}, \frac{r^2}{32\rho}\right)$, one has*

$$\left\| \mathcal{V}_{Z_h, R}(\chi) - \widehat{\mathcal{V}}_{Z_h, R}(\chi) \right\|_{\text{op}} = O\left[r^2 R^2 (\text{Lip}(\chi) R + \|\chi\|_{\infty}) h^{\frac{1}{2}} + r^2 R \|\chi\|_{\infty} h\right].$$

Proof. Step 1: The aim of the first step is to prove that

$$\mathcal{V}_{Z_h, R}(\chi) = \int_{\text{vox}(\Omega_h^R)} (x - p_{Z_h}(x))(x - p_{Z_h}(x))^{\mathbf{t}} \chi(p_{Z_h}(x)) dx + R^2 \|\chi\|_{\infty} O(hr^2).$$

Since $\text{vox}(\Omega_h^R) \subset Z_h^R$, one has

$$\begin{aligned} \mathcal{V}_{Z_h, R}(\chi) &= \int_{\text{vox}(\Omega_h^R)} (x - p_{Z_h}(x))(x - p_{Z_h}(x))^{\mathbf{t}} \chi(p_{Z_h}(x)) dx \\ &\quad + \int_{Z_h^R \setminus \text{vox}(\Omega_h^R)} (x - p_{Z_h}(x))(x - p_{Z_h}(x))^{\mathbf{t}} \chi(p_{Z_h}(x)) dx \end{aligned}$$

By using the facts that $\|x - p_{Z_h}(x)\| \leq R$, χ is bounded by $\|\chi\|_{\infty}$, and the support of χ is contained in the ball $\mathcal{B}_y(r)$ (see Figure 2), the second term of the previous equation is bounded by

$$R^2 \times \|\chi\|_{\infty} \times \mathcal{H}^3\left([Z_h^R \setminus \text{vox}(\Omega_h^R)] \cap p_{Z_h}^{-1}(\mathcal{B}_y(r))\right).$$

Now, we claim that $Z_h^R \cap p_{Z_h}^{-1}(\mathcal{B}_y(r)) \subset p_{\partial X}^{-1}(\mathcal{B}_y(2r))$. Indeed, let $x \in Z_h^R \cap p_{Z_h}^{-1}(\mathcal{B}_y(r))$. The fact that the Hausdorff distance between Z_h and ∂X is less than h implies that $x \in \partial X^{R+h}$. Now, since $h \leq R$, Lemma 4 implies that $\|p_{\partial X}(x) - p_{Z_h}(x)\| \leq \sqrt{8h\rho} + h$, which leads to

$$\|p_{\partial X}(x) - y\| \leq \|p_{\partial X}(x) - p_{Z_h}(x)\| + \|p_{Z_h}(x) - y\| \leq \sqrt{8h\rho} + h + r \leq 2r.$$

Now, we show that $Z_h^R \setminus \text{vox}(\Omega_h^R) \subset \partial X^{R+h} \setminus \partial X^{R-(\sqrt{3}+1)h}$. Indeed, as said just before, one has $Z_h^R \subset \partial X^{R+h}$. Furthermore, if $x \in \partial X^{R-(\sqrt{3}+1)h}$, then the fact that the Hausdorff distance between Z_h and ∂X is less than h implies that $x \in Z_h^{R-\sqrt{3}h}$. Let $c \in h(\mathbb{Z} + \frac{1}{2})^3$ be the center of a voxel containing x . The fact that $\text{diam}(\text{vox}(c)) = \sqrt{3}h$ implies that $\text{vox}(c) \subset Z_h^R$, and thus $x \in Z_h^R$. We then get $Z_h^R \setminus \text{vox}(\Omega_h^R) \subset \partial X^{R+h} \setminus \partial X^{R-(\sqrt{3}+1)h}$. We finally deduce that

$$[Z_h^R \setminus \text{vox}(\Omega_h^R)] \cap p_{Z_h}^{-1}(\mathcal{B}_y(r)) \subset [\partial X^{R+3h} \setminus \partial X^{R-3h}] \cap p_{\partial X}^{-1}(\mathcal{B}_y(2r)), \quad (1)$$

whose volume is bounded by $O(hr^2)$ by Proposition 3, which allows us to conclude.

Step 2: We then have to bound the remaining term

$$\Delta = \int_{\text{vox}(\Omega_h^R)} (x - p_{Z_h}(x))(x - p_{Z_h}(x))^{\mathbf{t}} \chi(p_{Z_h}(x)) dx - \widehat{\mathcal{V}}_{Z_h, R}(\chi).$$

By decomposing Δ over all the voxels of $\text{vox}(\Omega_h^R)$, one has

$$\Delta = \sum_{c \in \Omega_h^R} \int_{\text{vox}(c)} [(x - p_{Z_h}(x))(x - p_{Z_h}(x))^{\mathbf{t}} \chi(p_{Z_h}(x)) - (c - p_{Z_h}(c))(c - p_{Z_h}(c))^{\mathbf{t}} \chi(p_{Z_h}(c))] dx$$

As in Step 1, we can localise the calculation around the support of χ and we introduce the set of centers $D = \Omega_h^R \cap p_{\partial X}^{-1}(\mathcal{B}_y(2r))$. Using the relation $\chi(p_{Z_h}(c)) = \chi(p_{Z_h}(c)) + \chi(p_{Z_h}(x)) - \chi(p_{Z_h}(x))$, one gets $\Delta = \Delta_1 + \Delta_2$, where

$$\begin{aligned} \Delta_1 &= \sum_{c \in D} \int_{\text{vox}(c)} (x - p_{Z_h}(x))(x - p_{Z_h}(x))^{\mathbf{t}} [\chi(p_{Z_h}(x)) - \chi(p_{Z_h}(c))] dx \\ \Delta_2 &= \sum_{c \in D} \int_{\text{vox}(c)} [(x - p_{Z_h}(x))(x - p_{Z_h}(x))^{\mathbf{t}} - (c - p_{Z_h}(c))(c - p_{Z_h}(c))^{\mathbf{t}}] \chi(p_{Z_h}(c)) dx \end{aligned}$$

We are now going to bound Δ_1 and Δ_2 . One has

$$\|\Delta_1\|_{\text{op}} \leq \sum_{c \in D} \int_{\text{vox}(c)} \|x - p_{Z_h}(x)\| \|x - p_{Z_h}(x)\|^{\mathbf{t}} \|\chi(p_{Z_h}(x)) - \chi(p_{Z_h}(c))\| dx.$$

For all $c \in D$ and $x \in \text{vox}(c)$, we have $\|x - c\| \leq \frac{\sqrt{3}}{2}h$. Furthermore, by definition of Ω_h^R , we have that x and c belong to $Z_h^R \subset \partial X^{R+h}$. Then, since $h \leq R \leq \frac{\rho}{2}$, Proposition 4 implies $\|p_{Z_h}(x) - p_{Z_h}(c)\| = O(h^{\frac{1}{2}})$ and then $\|\chi(p_{Z_h}(x)) - \chi(p_{Z_h}(c))\| = \text{Lip}(\chi)O(h^{\frac{1}{2}})$. Using the fact that $\|x - p_{Z_h}(x)\| \leq R$, one has

$$\|\Delta_1\|_{\text{op}} = \text{Vol}(\text{vox}(D)) \times R^2 \times \text{Lip}(\chi) \times O(h^{\frac{1}{2}}).$$

Since $\text{vox}(D) \subset Z_h^R \cap p_{\partial X}^{-1}(\mathcal{B}_y(2r)) \subset \partial X^{R+h} \cap p_{\partial X}^{-1}(\mathcal{B}_y(2r))$ and $h \leq R$, Proposition 3 implies that $\text{Vol}(\text{vox}(D)) = O(r^2 R)$. Finally $\|\Delta_1\|_{\text{op}} = \text{Lip}(\chi) \times O(r^2 R^3 h^{\frac{1}{2}})$.

Similarly, let us bound $\|\Delta_2\|_{\text{op}}$. We put $u = (x - c)$, $v = c - p_{Z_h}(c)$ and $w = p_{Z_h}(c) - p_{Z_h}(x)$. We can write $x - p_{Z_h}(x) = u + v + w$, and we get

$$\Delta_2 = \sum_{c \in D} \left[\int_{\text{vox}(c)} [(u + v + w)(u + v + w)^t - vv^t] \chi(p_{Z_h}(c)) \right].$$

From $\|u\| \leq h$, $\|v\| \leq R$ and $\|w\| = O(h^{\frac{1}{2}})$, we bound the integrand by $O(\|\chi\|_{\infty} (R h^{\frac{1}{2}} + h))$. From $\text{Vol}(\text{vox}(D)) = O(r^2 R)$, one has $\|\Delta_2\|_{\text{op}} = O(\|\chi\|_{\infty} (R^2 r^2 h^{\frac{1}{2}} + r^2 R h))$.

Stability of the VCM. It is known that the VCM is stable. More precisely, Theorem 5.1 of [1] states that $\|\mathcal{V}_{\partial X, R}(\chi_r) - \mathcal{V}_{Z_h, R}(\chi_r)\|_{\text{op}} = O(h^{\frac{1}{2}})$. However, the constant involved in $O(h^{\frac{1}{2}})$ depends on the whole surface ∂X . We provide here a more precise constant involving only local estimations, r and R . The proof is very similar to the one of [1], except that we localise the calculation of the integral. It is given in Appendix.

Proposition 2. *For any $h \leq R$ such that $\sqrt{8h\rho} + h \leq r$, one has*

$$\begin{aligned} & \|\mathcal{V}_{\partial X, R}(\chi_r) - \mathcal{V}_{Z_h, R}(\chi_r)\|_{\text{op}} \\ &= O\left(\text{Lip}(\chi) \times [(r^3 R^{\frac{5}{2}} + r^2 R^{\frac{7}{2}} + r R^{\frac{9}{2}}) h^{\frac{1}{2}}] + \|\chi\|_{\infty} \times [(r^3 R^{\frac{3}{2}} + r^2 R^{\frac{5}{2}} + r R^{\frac{7}{2}}) h^{\frac{1}{2}}]\right). \end{aligned}$$

End of proof of Theorem 1. Let $h \leq \min\left(R, \frac{r}{2}, \frac{r^2}{32\rho}\right)$. The assumption $h \leq \frac{r^2}{32\rho}$ implies that $\sqrt{8h\rho} + h \leq r$. Thus we can apply Proposition 1 and Proposition 2.

3 Multigrid convergence of the normal estimator

Let X be a compact domain of \mathbb{R}^3 whose boundary ∂X is a surface of class C^2 . We now want to estimate the normal, denoted by $n(p_0)$, of ∂X at a point p_0 from its Gauss digitisation. We define the normal estimator by applying the digital VCM on a Lipschitz function that approaches the indicatrix of the ball $\mathcal{B}_{p_0}(r)$.

Definition 1. *The normal estimator $\hat{n}_{r, R}(p_0)$ is the unit eigenvector associated to the largest eigenvalue of $\hat{\mathcal{V}}_{Z_h, R}(\chi_r)$, where χ_r is a Lipschitz function that is: equal to 1 on $\mathcal{B}_{p_0}(r)$, equal to $1 - (\|x - p_0\| - r)/r^{\frac{3}{2}}$ on $\mathcal{B}_{p_0}(r + r^{\frac{3}{2}}) \setminus \mathcal{B}_{p_0}(r)$, and equal to 0 elsewhere.*

Remark that the normal estimator is defined only up to the sign. The following theorem gives an error estimation between $\pm \hat{n}_{r, R}(p_0)$ and $n(p_0)$.

Theorem 2. *Let X be a compact domain of \mathbb{R}^3 whose boundary ∂X is a C^2 surface with reach $\rho > 0$. Let $R < \frac{\rho}{2}$. Then for any $h > 0$ such that $h \leq \min\left(R, \frac{r}{2}, \frac{r^2}{32\rho}\right)$, the angle between the lines spanned by $\widehat{n}_{r,R}(p_0)$ and $n(p_0)$ satisfies*

$$\langle \widehat{n}_{r,R}(p_0), n(p_0) \rangle = O\left((rR^{-\frac{3}{2}} + R^{-1} + r^{-\frac{1}{2}}R^{-\frac{1}{2}} + r^{-\frac{3}{2}} + r^{-\frac{5}{2}}R^{\frac{3}{2}})h^{\frac{1}{2}} + R^{-2}h + r^{\frac{1}{2}} + R^2\right).$$

The following corollary is a direct consequence.

Corollary 1. *Let X be a compact domain of \mathbb{R}^3 whose boundary ∂X is a C^2 surface with reach $\rho > 0$. Let $a, b \in \mathbb{R}^+$, $r = ah^{\frac{1}{4}}$ and $R = bh^{\frac{1}{4}}$. Then for any $h > 0$ small enough, one has*

$$\langle \widehat{n}_{r,R}(p_0), n(p_0) \rangle = O\left(h^{\frac{1}{8}}\right).$$

Proof of Theorem 2. We introduce the normalized VCM $\widehat{N}_{r,R}(p_0) = \frac{3}{2\pi r^2 R^3} \widehat{\mathcal{V}}_{Z_h, R}(\chi_r)$. From Davis-Kahan $\sin(\theta)$ Theorem [11], up to the sign of $\pm \widehat{n}_{r,R}(p_0)$, one has

$$\|\widehat{n}_{r,R}(p_0) - n(p_0)\| \leq 2 \left\| \widehat{N}_{r,R}(p_0) - n(p_0)n(p_0)^t \right\|_{\text{op}}.$$

It is therefore sufficient to bound the right hand side. The triangle inequality gives

$$\begin{aligned} \left\| \widehat{N}_{r,R}(p_0) - n(p_0)n(p_0)^t \right\|_{\text{op}} &\leq \frac{3}{2\pi R^3 r^2} \left\| \widehat{\mathcal{V}}_{Z_h, R}(\chi_r) - \mathcal{V}_{\partial X, R}(\chi_r) \right\|_{\text{op}} \\ &\quad + \frac{3}{2\pi R^3 r^2} \left\| \mathcal{V}_{\partial X, R}(\chi_r) - \mathcal{V}_{\partial X, R}(\mathbf{1}_{\mathcal{B}_{p_0}(r)}) \right\|_{\text{op}} \\ &\quad + \left\| \frac{3}{2\pi R^3 r^2} \mathcal{V}_{\partial X, R}(\mathbf{1}_{\mathcal{B}_{p_0}(r)}) - n(p_0)n(p_0)^t \right\|_{\text{op}}. \end{aligned}$$

The proof of the theorem relies on Theorem 1, that controls the first term, and on the two following lemmas.

Lemma 1. *Under the assumption of Theorem 2, we have*

$$\frac{3}{2\pi r^2 R^3} \left\| \mathcal{V}_{\partial X, R}(\chi_r) - \mathcal{V}_{\partial X, R}(\mathbf{1}_{\mathcal{B}_{p_0}(r)}) \right\|_{\text{op}} = O(r^{\frac{1}{2}}).$$

Proof. Since $\chi_r = \mathbf{1}_{\mathcal{B}_{p_0}(r)}$ on the ball $\mathcal{B}_{p_0}(r)$, by using similar arguments as previously, one has

$$\left\| \mathcal{V}_{\partial X, R}(\chi_r) - \mathcal{V}_{\partial X, R}(\mathbf{1}_{\mathcal{B}_{p_0}(r)}) \right\|_{\text{op}} \leq \text{Vol} \left(\partial X^R \cap \left[p_{\partial X}^{-1}(\mathcal{B}_y(r + r^{\frac{3}{2}})) \setminus p_{\partial X}^{-1}(\mathcal{B}_y(r)) \right] \right) \times R^2.$$

Proposition 3 implies that the volume $\text{Vol} \left(\partial X^R \cap \left[p_{\partial X}^{-1}(\mathcal{B}_y(r + r^{\frac{3}{2}})) \setminus p_{\partial X}^{-1}(\mathcal{B}_y(r)) \right] \right)$ is less than $4R \times \text{Area} \left(\mathcal{B}_y(r + r^{\frac{3}{2}}) \setminus \mathcal{B}_y(r) \right)$. The fact that this area is bounded by $O(r^{\frac{5}{2}})$ allows to conclude.

Lemma 2. *Under the assumption of Theorem 2, we have*

$$\left\| \frac{3}{2\pi R^3 r^2} \mathcal{V}_{\partial X, R}(\mathbf{1}_{\mathcal{B}_{p_0}(r)}) - n(p_0)n(p_0)^t \right\|_{\text{op}} = O(r + R^2)$$

Proof. We have the following relation (see Theorem 1 of [12])

$$\mathcal{V}_{\partial X, R}(\mathbf{1}_{\mathcal{B}_{p_0}(r)}) = \frac{2}{3} R^3 [1 + O(R^2)] \int_{p \in \mathcal{B}_{p_0}(r) \cap S} n(p)n(p)^t \, dp. \quad (2)$$

By the mean value theorem applied to the normal to ∂X , one has

$$\|n(p) - n(p_0)\| \leq \sup_{q \in S} \|Dn(q)\|_{\text{op}} l_{p, p_0},$$

where l_{p, p_0} is the length of a geodesic joining p and p_0 . Since the chord (pp_0) belongs to the offset ∂X^R , where $R < \rho$, we have $l_{p, p_0} = O(\|p - p_0\|)$ (see [13] for example). Therefore $\|n(p) - n(p_0)\| = O(r)$ and thus $n(p)n(p)^t - n(p_0)n(p_0)^t = O(r)$. Consequently

$$\int_{p \in \mathcal{B}_{p_0}(r) \cap S} n(p)n(p)^t \, dp = \text{Area}(\mathcal{B}_{p_0}(r) \cap S) n(p_0)n(p_0)^t + \text{Area}(\mathcal{B}_{p_0}(r) \cap S) O(r).$$

Combining with Eq. (2), we have

$$\frac{3}{2R^3 \text{Area}(\mathcal{B}_{p_0}(r) \cap S)} \mathcal{V}_{\partial X, R}(\mathbf{1}_{\mathcal{B}_{p_0}(r)}) = [1 + O(R^2)] \times (n(p_0)n(p_0)^t + O(r)).$$

We conclude by using the fact that $\text{Area}(\mathcal{B}_{p_0}(r) \cap S)$ is equivalent to πr^2 .

4 Experiments

We evaluate experimentally the multigrid convergence, the accuracy and robustness to Hausdorff noise of our normal estimator, and also its ability to detect features.

The first series of experiments analyzes the convergence of the normal estimation by VCM toward the true normal of the shape boundary ∂X . The shape “torus” is a torus of great radius 6 and small radius 2, and the shape “ellipsoid” is an ellipsoid of half-axes $\sqrt{90}$, $\sqrt{45}$ and $\sqrt{45}$. We measure the absolute angle error with $\epsilon(p) = \frac{180}{\pi} \cos^{-1}(\hat{n}(p) \cdot n(p))$ for every point $p \in Z_h$ of the digitized shape with several normalized norms:

$$l_1(\epsilon) \stackrel{\text{def}}{=} \frac{1}{\text{Card}(Z_h)} \sum_{p \in Z_h} \epsilon(p), \quad l_\infty(\epsilon) \stackrel{\text{def}}{=} \sup_{p \in Z_h} \epsilon(p). \quad (3)$$

In experiments we tried several kernel functions χ_r and we display results for two of them: the “ball” kernel $\chi_{p_0, r}^0(x) = 1$ if $\|x - p_0\| \leq r$, 0 otherwise; the “hat” kernel $\chi_{p_0, r}^1(x) = 1 - \|x - p_0\|/r$ if $\|x - p_0\| \leq r$, 0 otherwise. Figure 3 displays the norms of the estimation angle error in degrees, for finer and finer digitization

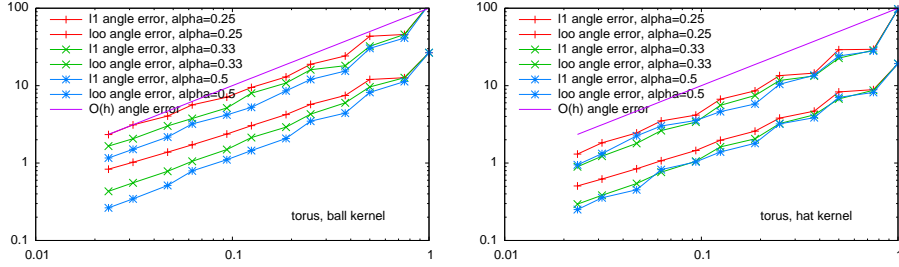


Fig. 3: Multigrid convergence of angle error of normal estimator (in degree). Abscissa is the gridstep h . Tests are run on torus shape for three kernel radii ($R = r = 3h^\alpha$ for $\alpha \in \{\frac{1}{4}, \frac{1}{3}, \frac{1}{2}\}$), two norms (l_1, l_∞): (left) kernel ball function χ_r^0 , (right) kernel hat function χ_r^1 .

steps. Corollary 1 predicts the multigrid convergence of the estimator when $r = ah^{\frac{1}{4}}$ and $R = bh^{\frac{1}{4}}$ at a rate in $O(h^{\frac{1}{8}})$. We observe the convergence of the estimator for parameters $R = r = 3h^{\frac{1}{4}}$, $R = r = 3h^{\frac{1}{3}}$, $R = r = 3h^{\frac{1}{2}}$, at an almost linear rate $O(h)$, for all norms. More experiments show that the most accurate results are obtained for $\alpha \in [\frac{1}{3}, \frac{1}{2}]$ if $R = r = ah^\alpha$. Note that the kernel function has not a great impact on normal estimates, as long as it has a measure comparable to the ball kernel.

We perturbate the shape “torus” with a Kanungo noise model of parameter $p = 0.25$ (the number p^d is the probability that a voxel at digital distance d from the boundary ∂X is flipped inside/out). This is not exactly a Hausdorff perturbation but most perturbations lie in a band of size $2h/(1-p)$. Figure 4 shows that the normal is still convergent for all norms. Again convergence speed is experimentally closer to $O(h^{\frac{2}{5}})$, much better than the proved $O(h^{\frac{1}{8}})$.

We then assess the visual quality of the estimators on several shapes, by rendering the digital surfels according to their estimated normals. First of all, Figure 5 displays normal estimation results on a noisy “torus” shape perturbed with a strong Kanungo noise of parameter $p = 0.5$. Then, Figure 6 displays the visual improvement of using normals computed by the VCM estimator. In particular, comparing Fig.6b and Fig.6c shows that convolving Voronoi cell geometry is much more precise than convolving only surfel geometry. Furthermore, we have tested our estimator on many classical digital geometry shapes (see Figure 7).

Our VCM estimator is a matrix and carries also curvature information along other eigendirections. Mérigot *et al.* [1] proposed to detect sharp features by using the three eigenvalues l_1, l_2, l_3 of the VCM as follows: if $l_1 \geq l_2 \geq l_3$, compute $l_2/(l_1 + l_2 + l_3)$ and mark the point as *sharp* if this value exceeds a threshold T . Figure 8 shows such sharp features detection on the “bunny” dataset at many different scales, with $T = 0.1$ for all datasets (it corresponds to an angle of $\approx 25^\circ$). This shows that the VCM information is geometrically stable and essentially scale-invariant. To conclude, we list below some information on computation times. This

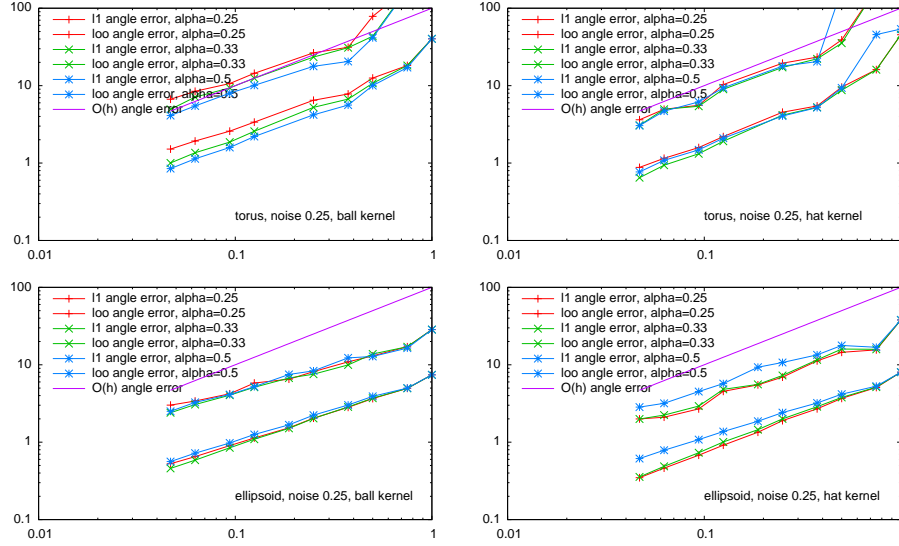


Fig. 4: Multigrid convergence of angle error of normal estimator (in degree) on a *noisy* shape. Abscissa is the gridstep h . Tests are run on “torus” shape (upper row) and on “ellipsoid” shape (lower row), perturbed by a Kanungo noise of parameter 0.25, for three kernel radii ($R = r = 3h^\alpha$ for $\alpha \in \{\frac{1}{4}, \frac{1}{3}, \frac{1}{2}\}$), two norms (l_1, l_∞): (left) kernel ball function χ_r^0 , (right) kernel hat function χ_r^1 .

estimator has been implemented using the DGtal library [14], and will soon be freely available in it.

Image	size	#surfels	(R, r)	χ_r -VCM	comput.	Orienting normals
“Al”	150^3	48017	(30, 3)	0.73 s		0.88 s
“rcruiser”	250^3	66543	(30, 3)	1.26 s		0.99 s
“bunny”	516^3	933886	(30, 5)	30.1 s		15.9 s
“Dig. Snow”	512^3	3035307	(30, 5)	82.1 s		53.6 s

5 Conclusion

We have presented new stable geometry estimators for digital data, one approaching the Voronoi Covariance Measure and the other approaching the normal vector field. We have shown under which conditions they are multigrid convergent and provided formulas to determine their parameters R and r as a function of the gridstep h . Experiments have confirmed both the accuracy and the stability of our estimators. In future works, we plan to compare numerically our estimator with other discrete normal estimators (e.g. integral invariants [7], jets [15]) and also to perform a finer multigrid analysis to get a better theoretical bound on the error.

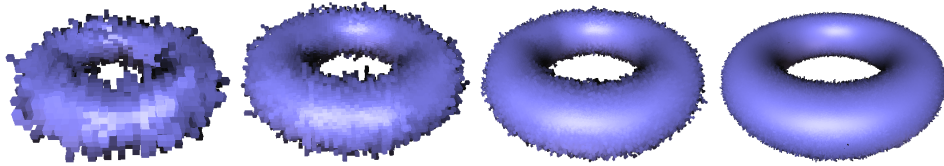


Fig. 5: Visual result of the normal estimation on the “torus” shape perturbed with a strong Kanungo noise ($p = 0.5$) for gridsteps from left to right $h = 0.5, 0.25, 0.125, 0.0626$.

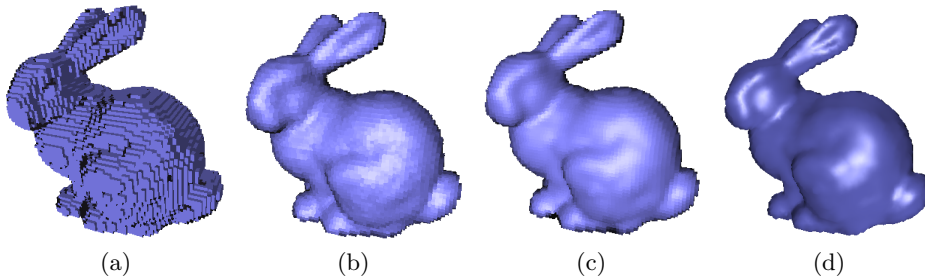


Fig. 6: Visual aspect of normal estimation on “bunny66” for $r = 3$: (a) trivial normals, (b) normals by χ_r^1 convolution of trivial normals with flat shading, (c) χ_r^1 -VCM normals with flat shading, (d) χ_r^1 -VCM normals with Gouraud shading.

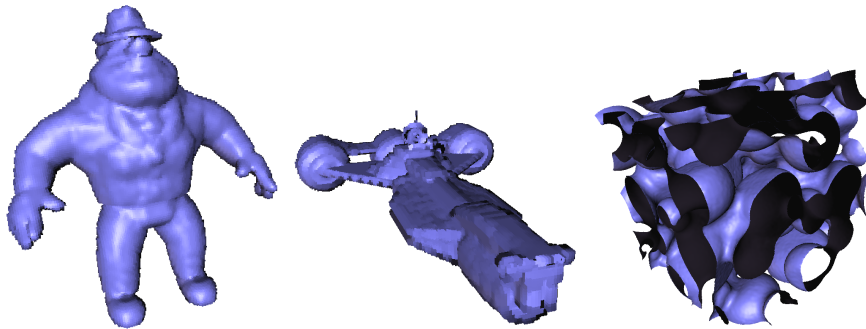


Fig. 7: Visual aspect of normal estimation on classical digital data structures: “Al” 150^3 , “Republic cruiser” 250^3 , “Digital snow” 512^3 .

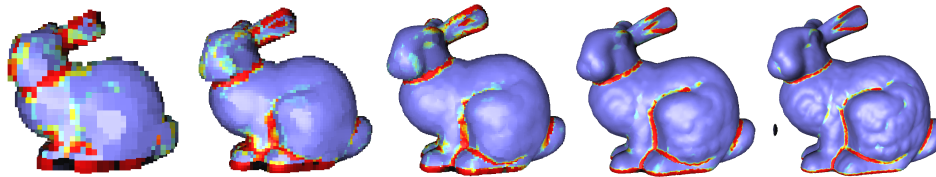


Fig. 8: Sharp feature detection on “bunny” dataset at increasing resolutions ($R = 30$, $T = 0.1$): color is metallic blue when value is in $[0, \frac{2}{3}T]$, then goes through cyan and yellow in $]\frac{2}{3}T, T[$, till red in $[T, +\infty[$.

References

1. Q. Mérigot, M. Ovsjanikov, and L. Guibas. Voronoi-based curvature and feature estimation from point clouds. *IEEE Transactions on Visualization and Computer Graphics*, 17(6):743–756, 2011.
2. F. de Vieilleville and J.O. Lachaud. Comparison and improvement of tangent estimators on digital curves. *Pattern Recognition*, 2008.
3. L. Provot and Y. Gérard. Estimation of the derivatives of a digital function with a convergent bounded error. In *Discrete Geometry for Computer Imagery (DGCI'2011)*, LNCS, pages 284–295. Springer, 2011.
4. B. Kerautret and J.O. Lachaud. Curvature estimation along noisy digital contours by approximate global optimization. *Pattern Recognition*, 2009.
5. T. Roussillon and J.O. Lachaud. Accurate curvature estimation along digital contours with maximal digital circular arcs. In *Combinatorial Image Analysis*, LNCS. 2011.
6. S. Fourey and R. Malgouyres. Normals and curvature estimation for digital surfaces based on convolutions. In *DGCI*, LNCS. Springer, 2008.
7. D. Coeurjolly, J.O. Lachaud, and J. Levallois. Integral based curvature estimators in digital geometry. In *DGCI*, LNCS. Springer, 2013.
8. F. Cazals and M. Pouget. Estimating differential quantities using polynomial fitting of osculating jets. *Computer Aided Geometric Design*, 22(2):121–146, 2005.
9. N. Amenta and M. Bern. Surface reconstruction by voronoi filtering. *Discrete & Computational Geometry*, 22(4):481–504, 1999.
10. P. Alliez, D. Cohen-Steiner, Y. Tong, and M. Desbrun. Voronoi-based variational reconstruction of unoriented point sets. In *Symposium on Geometry processing*, volume 7, page 3948, 2007.
11. C. Davis. The rotation of eigenvectors by a perturbation. *Journal of Mathematical Analysis and Applications*, 1963.
12. Q. Mérigot. *Détection de structure géométrique dans les nuages de points*. PhD thesis, Université Nice Sophia Antipolis, December 2009.
13. J.M. Morvan and B. Thibert. Approximation of the normal vector field and the area of a smooth surface. *Discrete & Computational Geometry*, 32(3):383–400, 2004.
14. DGTAL: Digital geometry tools and algorithms library, <http://libdgtal.org>.
15. F. Cazals and M. Pouget. Estimating differential quantities using polynomial fitting of osculating jets. *Computer Aided Geometric Design*, 22(2):121–146, February 2005.
16. H. Weyl. On the volume of tubes. *American Journal of Mathematics*, pages 461–472, 1939.
17. H. Federer. Curvature measures. *Trans. Amer. Math. Soc.*, 93(3):418–491, 1959.

Appendix

We give here all the proofs to be self-content. Proposition 3 is classical and follows from the well-known tube formula for smooth surfaces [16]. We give a complete proof in the sake of completeness. Proposition 4 states that the projection map p_K onto a set K that is close to a smooth surface S behaves like the projection map p_S . It relies on classical properties of the projection map onto a set with positive reach. The proof of Proposition 2 is similar to the proof of Theorem 5.1 of [1], except that the calculations are done locally.

5.1 Hausdorff measure of offsets

Proposition 3. *Let $S \subset \mathbb{R}^3$ be a surface of class C^2 with reach $\rho > 0$. Let $R > 0$ and $\varepsilon > 0$ be such that $R + \varepsilon < \frac{\rho}{2}$. Then for any borelian \mathcal{B} , one has:*

1. $\text{Vol}(S^R \cap p_S^{-1}(\mathcal{B} \cap S)) \leq 4 R \text{Area}(\mathcal{B} \cap S)$.
2. $\text{Vol}((S^{R+\varepsilon} \setminus S^{R-\varepsilon}) \cap p_S^{-1}(\mathcal{B} \cap S)) \leq 7 \varepsilon \text{Area}(\mathcal{B} \cap S)$.
3. $\text{Area}(\partial[S^R \cap p_S^{-1}(\mathcal{B} \cap S)]) \leq 3 R \text{Length}(\partial(\mathcal{B} \cap S)) + 5 \text{Area}(\mathcal{B} \cap S)$

In particular, if \mathcal{B} is a ball of radius r , one has:

- a. $\text{Vol}(S^R \cap p_S^{-1}(\mathcal{B} \cap S)) = O(Rr^2)$.
- b. $\text{Vol}((S^{R+\varepsilon} \setminus S^{R-\varepsilon}) \cap p_S^{-1}(\mathcal{B} \cap S)) = O(\varepsilon r^2)$.
- c. $\text{Area}(\partial[S^R \cap p_S^{-1}(\mathcal{B} \cap S)]) = O(Rr + r^2)$,

where the notation O involves a constant that only depends on the reach ρ .

Proof. The proof is based on the tube formula for surfaces of class C^2 [16, 17]. One has

$$\text{Vol}(S^R \cap p_S^{-1}(\mathcal{B} \cap S)) = \int_{\mathcal{B} \cap S} \int_{-R}^R (1 - t\lambda_1(x))(1 - t\lambda_2(x)) dt dx,$$

where $\lambda_1(x)$ and $\lambda_2(x)$ are the principal curvatures of S at the point x . Now, since $|\lambda_1(x)|$ and $|\lambda_2(x)|$ are smaller than $\frac{1}{\rho}$, one has

$$\text{Vol}(S^R \cap p_S^{-1}(\mathcal{B} \cap S)) \leq \int_{\mathcal{B} \cap S} dx \times \int_{-R}^R \left(1 + \frac{t}{\rho}\right)^2 dt \leq \text{Area}(\mathcal{B} \cap S) \times 2R \left(1 + \frac{R^2}{3\rho^2}\right).$$

The proof of the second item is similar. The volume of $(S^{R+\varepsilon} \setminus S^{R-\varepsilon}) \cap p_S^{-1}(\mathcal{B} \cap S)$ is less than

$$\int_{\mathcal{B} \cap S} dx \times \left[\int_{R-\varepsilon}^{R+\varepsilon} \left(1 + \frac{t}{\rho}\right)^2 dt + \int_{-R-\varepsilon}^{-R+\varepsilon} \left(1 - \frac{t}{\rho}\right)^2 dt \right]$$

The result then follows from the fact that

$$\int_{R-\varepsilon}^{R+\varepsilon} \left(1 + \frac{t}{\rho}\right)^2 dt = 2\varepsilon + \frac{2\varepsilon R}{\rho} + \frac{2\varepsilon(R+\varepsilon)^2}{\rho^2} \leq \frac{7}{2}\varepsilon.$$

For the last point, one has

$$\partial[S^R \cap p_S^{-1}(\mathcal{B} \cap S)] = A_1 \cup A_2,$$

where

$$\begin{aligned} A_1 &= \{x \in \mathbb{R}^3, \|x - p_S(x)\| = R \text{ and } p_S(x) \in \mathcal{B} \cap S\} \\ A_2 &= S^R \cap p_S^{-1}(\partial(\mathcal{B} \cap S)) \end{aligned}$$

Similarly as above, one has

$$\begin{aligned} \text{Area}(A_1) &= \int_{\mathcal{B} \cap S} (1 - \lambda_1(x)R)(1 - \lambda_2(x)R) dx \\ &\leq 2\text{Area}(\mathcal{B} \cap S) \left(1 + \frac{R}{\rho}\right)^2 \\ &\leq 5\text{Area}(\mathcal{B} \cap S). \end{aligned}$$

We put $\mathcal{C} = \partial[\mathcal{B} \cap S]$. As for the tube formula, the set A_2 is parametrized by the map

$$\begin{aligned} f : \mathcal{C} \times (-R, R) &\longrightarrow A_2 \\ (x, t) &\longmapsto x + t.n(x) \end{aligned}$$

The 2-jacobian of f at (x, t) is given by $\|1 - t\lambda_{\mathcal{C}}(x)\|$, where $\lambda_{\mathcal{C}}(x)$ is the curvature of S at x in the direction tangent to \mathcal{C} . One has

$$\text{Area}(A_2) = \int_{\mathcal{C}} \int_{-R}^R \|1 - t\lambda_{\mathcal{C}}(x)\| dx \leq \text{Length}(\mathcal{C}) \int_{-R}^R 1 + \frac{|t|}{\rho} dt \leq 3R \text{Length}(\mathcal{C}).$$

The proofs of items a, b and c follows from the fact that if \mathcal{B} is a ball of radius r , then $\text{Area}(\mathcal{B} \cap S) = O(r^2)$ and $\text{Length}(\mathcal{C}) = O(r)$.

5.2 Stability of the projection on a compact set

Proposition 4. *Let S be a surface of \mathbb{R}^3 of class C^2 whose reach is greater than $\rho > 0$. Let K be a compact set such that $d_H(S, K) = \varepsilon < 2\rho$, and $R < \rho$ a positive number. If x and x' are points of S^R such that $d(x, x') \leq \eta$, then :*

$$\|p_K(x) - p_K(x')\| \leq 2\sqrt{8\varepsilon\rho} + 2\varepsilon + \frac{1}{1 - \frac{R}{\rho}}\eta$$

The proof of the proposition relies on Lemmas 3 and 4.

Lemma 3. *Let S be a surface of \mathbb{R}^3 of class C^2 whose reach is greater than $\rho > 0$. Let $r < \rho$ and $x \in \mathbb{R}^3$ such that $d(x, S) = \delta < \rho$. If $q \in S$ satisfies $\|q - p_S(x)\| > r$ then $\|x - q\|^2 > \frac{\delta}{\rho}r^2 + \delta^2$.*

Proof. Since S has a reach greater than ρ , there exists a ball $\mathcal{B}_c(\rho)$ of center c , that is tangent to S at the point $p_S(x)$. The interior of this ball does not intersect S and the points c , x , and $p_S(x)$ are aligned. Let q be a point of S such that $\|q - p_S(x)\| = \bar{r} \geq r$. We denote by \mathcal{P} the plane passing through c , x , $p_S(x)$ and p . Let $y \in \partial\mathcal{B}_c(\rho) \cap \partial\mathcal{B}_{p_S(x)}(\bar{r}) \cap \mathcal{P}$. Clearly, $p_S(x)$ is at equal distance of q and y . Furthermore, since $q \notin \mathcal{B}_c(\rho)$, c is closer to y than to q , hence the whole segment $[c, p_S(x)]$ is closer to y than to q , which implies that $\|x - q\| \geq \|x - y\|$. Since $\|x - y\|$ is the length of the diagonal of a regular trapezoid, we have $\|x - y\|^2 \geq \frac{\delta}{\rho}\bar{r}^2 + \delta^2$, which allows to conclude.

Lemma 4. *Let S be a surface of \mathbb{R}^3 with a reach $\rho > 0$. Let K be a compact set such that $d_H(S, K) = \varepsilon$ with $\varepsilon \leq 2\rho$. Let R be a number such that $R < \rho$. For every $x \in S^R$, one has*

$$p_K(x) \in B(p_S(x), \sqrt{8\varepsilon\rho} + \varepsilon)$$

Proof. Let $x \in S^R$. We denote $\delta = \|x - p_S(x)\|$. There exists $p_0 \in K$ such that $\|p_S(x) - p_0\| < \varepsilon$. We then have $\|x - p_0\| \leq \|x - p_S(x)\| + \|p_S(x) - p_0\| \leq \delta + \varepsilon$, which implies that $\|x - p_K(x)\| \leq \delta + \varepsilon$. Let now $p \in K$ be such that $p \notin B(p_S(x), \sqrt{8\rho\varepsilon} + \varepsilon)$. We are going to prove that $p \neq p_K(x)$.

We first suppose that $\delta < \varepsilon$. The assumption $\varepsilon \leq 2\rho$ implies that $3\varepsilon < \sqrt{8\rho\varepsilon} + \varepsilon$ and thus $\|p - p_S(x)\| \geq 3\varepsilon$. We have

$$\|x - p\| > \|p - p_S(x)\| - \|p_S(x) - x\| > 3\varepsilon - \delta > 2\varepsilon \geq \|x - p_K(x)\|,$$

which ensures that $p \neq p_K(x)$.

We now suppose that $\delta \geq \varepsilon$. There exists $q \in S$ such that $\|\tilde{p} - p\| \leq \varepsilon$ and thus $\|q - p_S(x)\| \geq \sqrt{8\rho\varepsilon}$. Lemma 3 therefore implies that $\|x - q\|^2 > \frac{\delta}{\rho} \times 8\rho\varepsilon + \delta^2$. The fact that $\delta \geq \varepsilon$ implies that $\|x - q\| > \delta + 2\varepsilon$. We finally get $\|x - p\| \geq \|x - q\| - \varepsilon > \delta + \varepsilon \geq \|x - p_K(x)\|$, which ensures that $p \neq p_K(x)$.

Proof (of Proposition 4). By the triangle inequality, we have

$$\|p_K(x) - p_K(x')\| \leq \|p_K(x) - p_S(x)\| + \|p_S(x) - p_S(x')\| + \|p_S(x') - p_K(x')\|.$$

It is well-known that the projection map p_S is $\frac{1}{1-\frac{R}{\rho}}$ -Lipschitz in S^R (Theorem 4.8 of [17]). We then have $\|p_S(x) - p_S(x')\| \leq \frac{1}{1-\frac{R}{\rho}}\eta$. The two other terms are bounded with Lemma 4.

5.3 Proof of Proposition 2

As in the proof of the previous lemma, the hypothesis $h \leq \frac{\rho}{2}$ and $\sqrt{8h\rho} + h \leq r$ imply that $p_{Z_h}^{-1}(\text{supp}(\chi)) \subset p_{\partial X}^{-1}(\mathcal{B}_y(2r))$. We then introduce the common set $E = \partial X^{R-h} \cap p_{\partial X}^{-1}(\mathcal{B}_y(2r))$, on which we are going to integrate. We have :

$$\begin{aligned} \mathcal{V}_{\partial X, R}(\chi_r) &= \int_{\partial X^R} (x - p_{\partial X}(x))(x - p_{\partial X}(x))^{\mathbf{t}} \chi(p_{\partial X}(x)) \\ &= \int_{\partial X^R \cap p_{\partial X}^{-1}(\mathcal{B}_y(2r))} (x - p_{\partial X}(x))(x - p_{\partial X}(x))^{\mathbf{t}} \chi(p_{\partial X}(x)) \\ &= \int_E (x - p_{\partial X}(x))(x - p_{\partial X}(x))^{\mathbf{t}} \chi(p_{\partial X}(x)) + Err_1, \end{aligned}$$

where the error Err_1 satisfies

$$\|Err_1\|_{\text{op}} \leq R^2 \times \|\chi\|_{\infty} \times \text{Vol}(\partial X^R \cap p_{\partial X}^{-1}(\mathcal{B}_y(2r)) \setminus E).$$

Furthermore, one has $\partial X^R \cap p_{\partial X}^{-1}(\mathcal{B}_y(2r)) \setminus E = [\partial X^R \setminus \partial X^{R-h}] \cap p_{\partial X}^{-1}(\mathcal{B}_y(2r))$, whose volume is bounded by Proposition 3 by $O(r^2h)$. Then

$$\|Err_1\|_{\text{op}} = \|\chi\|_{\infty} \times O(R^2r^2h).$$

Similarly, one has

$$\begin{aligned} \mathcal{V}_{\partial X, R}(\chi_r) &= \int_{Z_h^R} (x - p_{Z_h}(x))(x - p_{Z_h}(x))^{\mathbf{t}} \chi(p_{Z_h}(x)) \\ &= \int_{Z_h^R \cap p_{\partial X}^{-1}(\mathcal{B}_y(2r))} (x - p_{Z_h}(x))(x - p_{Z_h}(x))^{\mathbf{t}} \chi(p_{Z_h}(x)) \\ &= \int_E (x - p_{Z_h}(x))(x - p_{Z_h}(x))^{\mathbf{t}} \chi(p_{Z_h}(x)) + Err_2, \end{aligned}$$

where the error Err_2 satisfies

$$\|Err_2\|_{\text{op}} \leq (R+h)^2 \times \|\chi\|_{\infty} \times \text{Vol}(Z_h^R \cap p_{\partial X}^{-1}(\mathcal{B}_y(2r)) \setminus E).$$

Since the set $Z_h^R \cap p_{\partial X}^{-1}(\mathcal{B}_y(2r)) \setminus E \subset [\partial X^{R+h} \setminus \partial X^{R-h}] \cap p_{\partial X}^{-1}(\mathcal{B}_y(2r))$ has a volume bounded by $O(r^2h)$, one has

$$\|Err_2\|_{\text{op}} = (R+h)^2 \times \|\chi\|_{\infty} \times O(r^2h).$$

We now have to compare the two integrals on the common set E

$$\Delta = \int_E [(x - p_{\partial X}(x))(x - p_{\partial X}(x))^{\mathbf{t}} \chi(p_{\partial X}(x)) - (x - p_{Z_h}(x))(x - p_{Z_h}(x))^{\mathbf{t}} \chi(p_{Z_h}(x))].$$

Following now the proof of Theorem 5.1 of [1], one has

$$\|\Delta\|_{\text{op}} \leq (R^2 \text{Lip}(\chi) + 2R\|\chi\|_{\infty}) \times [\text{Vol}(E) + (\text{diam}(E) + R + \sqrt{Rh}) \times \text{Area}(\partial E)] \times \sqrt{Rh}.$$

Proposition 3 gives that $\text{Vol}(E)$ is bounded by $O(r^2R)$ and $\text{Area}(\partial E)$ is bounded by $O(rR + r^2)$. We then have

$$\|\Delta\|_{\text{op}} = O\left(\text{Lip}(\chi) \times [(r^3R^{\frac{5}{2}} + r^2R^{\frac{7}{2}} + rR^{\frac{9}{2}})h^{\frac{1}{2}}] + \|\chi\|_{\infty} \times [(r^3R^{\frac{3}{2}} + r^2R^{\frac{5}{2}} + rR^{\frac{7}{2}})h^{\frac{1}{2}}]\right).$$

Adding the bounds of $\|Err_1\|_{\text{op}}$, $\|Err_2\|_{\text{op}}$ and $\|\Delta\|_{\text{op}}$, we find the same bound :

$$\begin{aligned} &\|\mathcal{V}_{\partial X, R}(\chi_r) - \mathcal{V}_{Z_h, R}(\chi_r)\|_{\text{op}} \\ &= O\left(\text{Lip}(\chi) \times [(r^3R^{\frac{5}{2}} + r^2R^{\frac{7}{2}} + rR^{\frac{9}{2}})h^{\frac{1}{2}}] + \|\chi\|_{\infty} \times [(r^3R^{\frac{3}{2}} + r^2R^{\frac{5}{2}} + rR^{\frac{7}{2}})h^{\frac{1}{2}}]\right). \end{aligned}$$